

MHD REGIMES AND FEEDBACK STABILIZATION IN ADVANCED TOKAMAKS

N. POMPHREY¹, S.C. JARDIN¹, J. BIALEK¹, M.S. CHANCE¹,
D.A. D'IPPOLITO², J.M. FINN³, R. FITZPATRICK⁴, J.L. JOHNSON¹,
C.E. KESSEL¹, J. MANICKAM¹, D.A. MONTICELLO¹, J.R. MYRA²,
M. ONO¹, W. PARK¹, A.H. REIMAN¹, G. REWOLDT¹, W.M. TANG¹,
E.J. VALEO¹, L.E. ZAKHAROV¹

¹Plasma Physics Laboratory,
Princeton University,
Princeton, New Jersey

²Lodestar Research Corporation,
Boulder, Colorado

³Los Alamos National Laboratory,
Los Alamos, New Mexico

⁴Institute for Fusion Studies,
University of Texas,
Austin, Texas

United States of America

Abstract

MHD REGIMES AND FEEDBACK STABILIZATION IN ADVANCED TOKAMAKS.

Various schemes are presented for improving the performance of tokamaks. These schemes attempt to maximize β while obtaining a high value of bootstrap current fraction. General principles are presented for guiding a search for such configurations. Several solutions are illustrated by ARIES and negative shear configurations. These attractive configurations rely on ideal wall stabilization of the low- n free boundary modes. Real walls, however, are three-dimensional and resistive and the paper addresses the theoretical treatment of these real three-dimensional and resistive walls. First, progress on a PEST/SPARK coupled code for treating three-dimensional walls is presented. This new code significantly extends the capability of PEST to allow an assessment of the stabilizing influence of a perfectly conducting wall with arbitrary poloidal and toroidal variation. Secondly, resistive walls are considered. A new mechanism for stabilizing the resistive wall mode is presented. This mechanism relies on plasma rotation, viscosity, and inertia. A stable window in the position of the resistive wall, similar to that demonstrated by Bondeson and Ward, is shown to exist for reasonable values of the rotation frequency. In addition, consideration of resistivity at the mode rational surface also leads to a stable window. Lastly, an active feedback stabilization scheme is considered for those cases where complete stabilization by the three-dimensional resistive wall is not possible. This feedback scheme relies on modulating the ponderomotive force of radiofrequency waves. A model calculation provides insight into the optimal antenna and detector arrangements.

1. MHD Regimes for Advanced Steady State Fusion Reactors

The Troyon stability limit, which is normally written as $\beta < C_T I_p / aB$, where $C_T = 3.5$, can also be expressed in the form

$$(\epsilon\beta_p)(\beta/\epsilon) < (C_T/20)^2(1 + \kappa^2)/2$$

where κ is the plasma elongation. This form clearly shows the tradeoff between β and β_p . The condition for efficient current drive is that $\epsilon\beta_p \sim 1$. This implies low β/ϵ values unless the Troyon limit is exceeded by achieving $\beta_N > C_T$. The goal of the steady state reactor is to use current drive to produce favorable plasma current profiles which allow increasing β_N and β_{*N} values (~ 1) which maximize the bootstrap fraction.

There are general principles that serve to guide the search for high β , high bootstrap fraction plasmas. For ballooning mode stability in the first regime, we want high shear everywhere. Broad pressure profiles normally lead to the highest stable values of β , but not always to the highest values of β_* . Triangularity is always found to be stabilizing in elongated plasmas.

For ballooning mode stability in the second regime, we know we need low, but non-zero, magnetic shear near the center. Negative shear is very stable. Peaked pressure profiles are normally necessary for access into full second stability, as is the condition $q_0 > 2$, and sufficient triangularity. Non-zero values of edge current improve edge accessibility.

For free-boundary $n = 1$ (kink mode) stability, we want high magnetic shear near the edge, or alternatively low values of edge current. It is known that the maximum stable β value increases with the internal inductance ℓ_i for fixed plasma current I_p and q_0 . Large values of q_* and large ℓ_i lead to the highest values of β_N , but not necessarily the highest values of β_* . There is no second stability for the $n = 1$ kink mode.

There are also general principles that guide us in seeking high bootstrap fraction configurations. In order to obtain $I_{bs}/I_p \sim 1$ normally requires a value of $\epsilon\beta_p \sim 1$. At fixed values of $\epsilon\beta_p$, the bootstrap fraction increases as the current profile is flattened (or q_*/q_0 is lowered), and as the density is peaked. Good bootstrap alignment normally requires both peaked pressure profiles and flat current profiles.

We find that for a first stability regime plasma, it is not possible to exceed bootstrap fractions of $I_{bs}/I_p \sim 0.7$ for conventional plasma profiles. The second stability regime is more compatible with high values of bootstrap fraction. It is possible to find at least two classes of configurations with $I_{bs}/I_p > 0.9$; one with a centrally peaked current profile and with $q_0 \sim 2$ and $\beta_N \sim 5$, and one with the current peaked off axis with negative central magnetic shear and with $\beta_N \sim 5$.

There are at least 4 configurations that have been proposed as potential steady state reactors: The ARIES-I reactor ($q_0 = 1.3$, $q_* = 3.9$, $\beta = 1.9\%$, $I_{bs}/I_p = 0.68$, $A = 4.5$)[1] represents a compromise between high β and high bootstrap fraction, while being constrained to be in first stability. It is stable to all MHD modes without a conducting wall.

The ARIES-II configuration [1] has sufficient elevated central safety factor, and sufficiently peaked pressure profile that it can exist in the second stability regime and thereby have simultaneously high values of β and β_p . The ARIES-II configuration has $q_0 = 2.0$, $q_* = 4.6$, $\beta = 3.4\%$, $I_{bs}/I_p = 0.98$, $A = 4.0$, however a nearby conducting wall located at $b/a = 1.3$ is necessary to stabilize the low- n MHD modes. The ARIES-III configuration ($q_0 = 2.0$, $q_* = 2.2$, $\beta = 24\%$, $I_{bs}/I_p = 1.16$, $A = 4.0$) which utilizes advanced fuels, has high β values, far into the second stability regime, but it requires plasma profiles with pressure gradients which remain finite out to the plasma edge, and with finite edge plasma current density [2]. It also requires an extremely close conducting wall to stabilize the $n = 1$ kink mode.

A configuration with a non-monotonic q profile[3] appears to offer significant advantages over the normal second-stability profiles. This mode maximizes β_* by distributing the plasma current to give negative magnetic shear and second stability in the central region. Off-axis current peaking and high- β allows for a very good match of the bootstrap and the equilibrium current profiles, and an attractive configuration is found with $q_0 = 2.5$, $q_* = 2.35$, $q_{min} = 2.1$ at $r/a \sim 0.75$, $\beta = 4.8\%$, $I_{bs}/I_p \sim 1$, $A = 4.5$. This configuration is a combination of both 1st and 2nd stability, but requires a conducting wall at about $1.3a$ to provide for kink mode stability. For these profiles the stability limit would decrease from $\beta_N = 5$ to $\beta_N = 2$ if the conducting wall were not present. Additional analysis indicates that this configuration is stable to resistive modes, and is stable to kinetic instabilities in regions where the pressure gradient is large [3].

2. PEST/SPARK Coupling for δW Analysis with 3D Ideal Walls

The attractive configurations discussed above rely on wall stabilization of the low- n free boundary modes. Stability calculations are typically performed using a perfectly conducting axisymmetric wall similar in shape, and concentric with, the plasma-vacuum interface. Real tokamak walls, however, are intrinsically three-dimensional and resistive, and we should understand the influence of these factors on free boundary instabilities.

To analyze ideal time-scale stabilization quantitatively, the PEST-VACUUM codes have been coupled to the 3D SPARK electromagnetics code, suitably modified to calculate the perturbed magnetic field from the induced wall currents using the PEST perturbations as its driver[4]. For each surface poloidal harmonic of the PEST displacement, the SPARK code is used to find the 3D magnetic perturbation, $\delta \mathbf{B}_s$, which, when driven by the fields obtained from PEST, combine with them to satisfy the appropriate boundary conditions at the 3D shell. The traditional PEST treatment for 2D vacuum-wall systems solves Laplace's equation for the magnetic scalar potential using collocation techniques for the integral equations generated by Green's second identity. The effects of the wall are incorporated directly into the resolving matrix for the potential. Now, for 3D wall systems, the vacuum treatment is reformulated into several steps to linearly superpose distinct contributions coming from a) the plasma *in the absence of the*

shell and from b) the shell *in the absence of the plasma* but driven by the plasma perturbations, while ensuring that the boundary conditions are appropriately taken on the *total* magnetic field. A modified vacuum energy matrix is finally calculated which is spectrally filtered in ϕ for input to PEST.

The SPARK code is used for step b) for eventual 3D applications. Meanwhile, it has been verified in a cylindrical limit (where vacuum fields are easily analysed in terms of Bessel functions), and in a toroidal case with poloidal cuts in an axisymmetric shell, that the new vacuum PEST algorithm gives identical results compared with the traditional PEST treatment. The coupled PEST/SPARK code significantly extends the capability of PEST to allow an assessment of the stabilizing influence of a perfectly conducting wall with arbitrary poloidal and toroidal variation.

3. Resistive Wall Mode Stabilization

Bondeson and Ward[5] have recently demonstrated the existence of a narrow window for placement of a resistive wall which results in complete stabilization of β driven external kinks. The stabilization, which requires sonic rotation, is

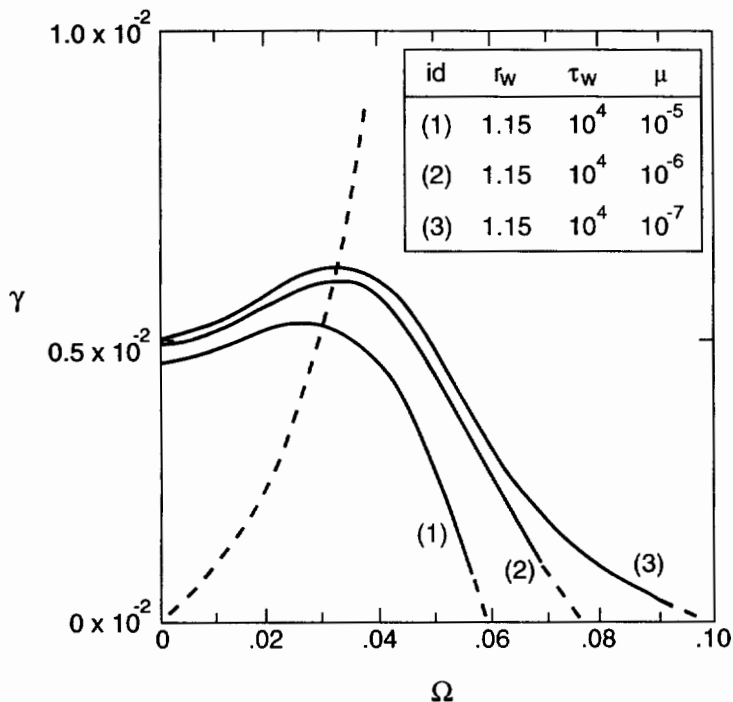


FIG. 1. Growth rate γ versus wall rotation frequency Ω for various viscosities (fixed resistive wall location r_w and time constant τ_w).

ascribed to toroidal coupling of the plasma perturbation to sound waves and Landau damping. The interesting possibility of complete stabilization has encouraged a consideration of additional damping mechanisms which can increase the size of the stable window.

The MH3D code is an initial value, nonlinear, 3D toroidal, resistive, compressible MHD code which is currently being used to study the stabilization of external kink modes. In the present application, a high conductivity plasma "core" region is surrounded by a low temperature resistive mantle, too resistive to carry any significant perturbed current. Plasma flows are allowed in the mantle as well as the core. Anomalous viscosity is included in the momentum equation, with viscosity, μ , a prescribed function of radius. Outside the mantle is a resistive (thick) wall at which slip conditions for the flow velocity are applied. Beyond the wall is a vacuum region which extends to a computational boundary where $\vec{B} \cdot \hat{n} = 0$. MH3D calculates and perturbs around equilibria with sheared toroidal mass flow, or can employ a rotating resistive wall.

To understand the physics of viscosity/inertia stabilization with rotation we will examine results for a cylindrical plasma model and a rotating resistive wall. Figures 1 and 2 present typical results, showing plots of linear growth rate, γ ,

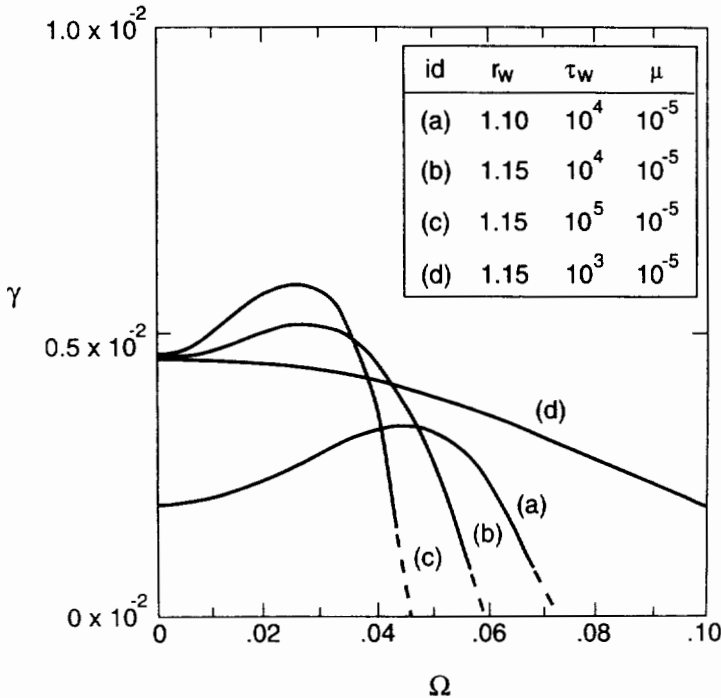


FIG. 2. Growth rate γ versus wall rotation frequency Ω for various resistive wall positions r_w and wall time constants τ_w at fixed viscosity.

versus wall rotation frequency, Ω , for a single helicity $m/n = 2/1$ external kink resistive wall mode, at zero beta. (Toroidal calculations with aspect ratio 5 show similar results). The equilibrium current profile is $J \sim (1 - r^2)^\nu$, with ν chosen to give $q_0 = 0.89$ and $q_1 = 1.80$. The $q = 2$ rational surface lies at $r_s = 1.05$ and the critical radius at which a perfectly conducting wall stabilizes the kink is $r_c = 1.20$. Results are shown for various resistive wall positions, r_w , plasma-mantle viscosities, μ , and wall time constants, τ_w . All variables are non-dimensionalized by scaling length and time with respect to minor radius and Alfvén time, respectively.

In Fig. 1 we show the dependence of growth rate on wall rotation frequency for three values of viscosity, μ . The resistive wall position and time constant are fixed, and $\mu_{core} = \mu_{mantle} = const$ for each curve. Consider first curve (1) corresponding to $\mu = 10^{-5}$, a value consistent with typical plasma edge parameters. Rotation is initially destabilizing; however increased slippage between the mode and wall frequencies (see dashed curve for mode frequency) causes a roll-over in γ vs. Ω , and complete stabilization is obtained at $\Omega_{crit} \approx 0.06$. Curves (2) and (3) show that decreasing the viscosity makes stabilization by rotation more difficult. In fact, by decreasing q_1 slightly we find that the modified curve (3) flattens out after the early roll-over, and complete stabilization is no longer obtained even for wall frequencies of order the Alfvén frequency. By varying the viscosity profile, it is found that it is μ at the edge of the plasma core, rather than μ in the mantle, that dominates the stabilization of the resistive wall mode. The resistive wall eigenfunctions show the importance of the restriction on plasma motion caused by the mantle inertia: the mantle allows flows which restrict the edge core plasma displacement, leading to stabilizing edge eddy currents.

Comparing curves (a) and (b) in Fig. 2 shows the effect of changing the resistive wall position, holding the wall time constant and plasma core/mantle viscosity constant. For zero wall rotation, of course, the mode growth rate is smallest for the resistive wall placed closest to the core plasma. However, mode slippage (an effect due to viscosity and inertia) is obtained more readily for the wall at $r_w = 1.15$ (closer to r_c) than it is for $r_w = 1.10$. This leads to a crossover of the curves of γ vs. Ω and complete stabilization of the wall mode at a smaller Ω_{crit} . Finally, in Fig. 2, curves (d), (b), and (c) show the effect on Ω_{crit} of increasing the wall time constant (curves (c) and (d) have been normalized to give the same growth rate as curve (b) at $\Omega = 0$). A deterioration in the ability of rotation to stabilize the the wall mode is seen as the wall conductivity is degraded.

Using the linearized incompressible equations of reduced MHD and treating the resistive wall in the "thin wall" limit, a dispersion relation may be derived which exhibits good qualitative, and fair quantitative agreement with the MH3D results, and provides additional understanding of the role of viscosity in stabilizing wall modes in the presence of rotation. In the regime of relevance to the MH3D calculations, the mantle is assumed to be too cold to carry any perturbed current. A viscous/inertial layer forms in the outer regions of the hot plasma.

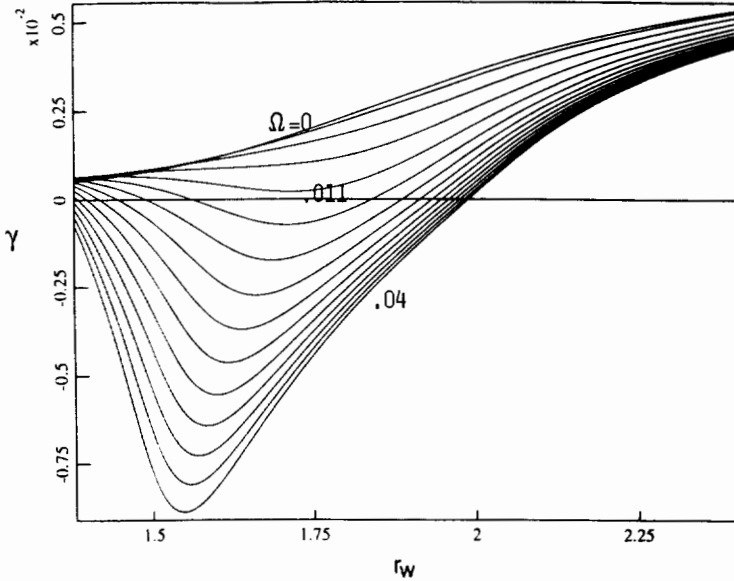


FIG. 3. Growth rate γ of a resistive wall-resistive external kink mode as a function of wall position r_w for 15 equally spaced values of Doppler shift frequency Ω between 0 and 0.04.

This layer can modify the magnetic eigenfunctions and lead to stabilization. The analysis reduces to usual asymptotic matching of "outer" magnetic eigenfunctions to "inner" layer solutions. The two layers are the edge region of the plasma and the resistive wall.

Under certain circumstances the kink mode dispersion relation reduces to a simple cubic. One of the roots is uninteresting because it is always stable. The two remaining roots are identified as the ideal external kink and resistive wall modes. At sufficiently high plasma rotation rates the regular resistive wall mode is stabilized and the ideal mode is almost marginally stable with inertia balancing the free energy (i.e., Δ') term in the dispersion relation. The mode is slightly destabilized by the wall resistivity and slightly stabilized by viscosity. For sufficiently long wall constants viscosity is dominant and the mode is stabilized.

Finally, we return to consideration of a cold mantle surrounding the hot core, but this time take into account the perturbed plasma currents in the mantle tearing layer[6]. This can lead to significant additional stabilization with rotation present[7, 8].

Several aspects of the stabilization of this resistive version of the kink mode can be understood in terms of a simple cylindrical model. For zero β , growth rates for a step function current density model with a resistive wall and rotation are shown in Fig. 3. For this case, $q_0 = q_1 = 1.05$, $m = 2$, $n = 1$, $\tau_w^{-1} = 0.0005$, and $\gamma_t = 0.01$, where γ_t is the tearing mode growth rate with the wall at infinity.

The $q = 2$ surface lies at $r_s = 1.38$ and disappears from the plasma for wall positions $r_w < r_s$. The ideal wall mode is unstable for $r_w > r_c = 2.11$. Figure 3 shows the growth rate as a function of wall position for 15 equally spaced values of the wall rotation frequency Ω between zero and 0.04. It is seen that a stable gap in r_w exists for Ω/γ_t of order unity, and for $\Omega/\gamma_t \gg 1$ the gap consists of almost the whole interval $r_s < r_w < r_c$. For $\Omega \sim \omega_*$ and T_e a few hundred eV, Ω/γ_t is of order unity. For hot plasmas $\Omega/\gamma_t \sim T_e^{1.9}$ is large. Unlike the results of Ref.[5], the stability gap is not associated with separation of the ideal wall and resistive wall modes. For example, for the parameters shown in Fig. 3, there is no mode crossing, although crossings can occur for negative γ [9]. For finite β in a cylinder the ideal kink can be unstable with a mode rational surface in the core plasma, unlike the case with zero β . For r_w, q_0 , and Ω fixed, as β decreases the mode passes through the following regimes: (i) unstable with ideal plasma and wall, with a mode rational surface in the plasma, (ii) below the ideal plasma threshold, but unstable as a resistive plasma mode, with ideal wall, (iii) below the threshold for resistive plasma instability with an ideal wall, but unstable as a resistive plasma-resistive wall mode, and (iv) a resistive plasma-resistive wall mode stabilized by rotation (i.e. in the stability gap of Fig. 3.)

In a torus, the major influences which must be taken into account relate to the width of the poloidal mode number m spectrum, the dominant m and Ω/γ_t at $q = m/n$. First, in the presence of sufficient rotation shear, the resistive plasma kink will have a narrower m spectrum[10] and the dominant m will depend on the profiles of resistivity and Ω . This narrowing causes the β limit of the mode to be closer to that of the ideal plasma mode than in the case with unsheared rotation. This limit may well be sufficiently close to the ideal threshold that it is within the experimental errors. There will be a large stability gap if $\Omega/\gamma_t > 1$ at $q = m/n$.

This type of resistive wall stabilization can also occur for current driven modes in toroidal geometry, and in particular can occur for zero β , unlike stabilization by coupling to sound waves.

4. Ponderomotive Feedback Stabilization of External Kinks

We have analyzed an active feedback scheme for MHD mode control using the modulated ponderomotive force (PF) of an array of radiofrequency (rf) antennas as the active stabilizing element. The dominant contribution to the PF is proportional to the product of the radial derivative of the plasma dielectric and the square of the slow wave rf field, which is modulated in response to an MHD mode detection system. The eigenmode equation for external kinks[11] has been modified to incorporate this PF feedback scheme, and feedback models have been formulated which represent two general types of feedback: A "local" response model where each antenna responds to the real-space plasma displacement measured locally (summed over all Fourier modes), and a "Fourier" response model where the antenna system is programmed to respond to a particular Fourier mode

(or superposition of modes). Numerical marginal stability calculations have been carried out in the cylindrical tokamak kink model to study the parametric dependences of each feedback system, and it is shown that the Fourier mode response is generally superior. The model calculations provide insight into the optimal antenna and detector arrangements, and preliminary rf power estimates have been made for stabilization of the $n=1$, low- m kinks on PBX-M, TPX and ITER. These estimates suggest that PBX-M would be able to do proof-of-principle $n=1$ kink stabilization experiments with the present system of two IBW antennas and available power supplies. Finally, rf and MHD issues critical to further development of this stabilization technique have been identified for future study.

A preliminary $n = 0$, $m = 1$ modulation experiment is planned on PBX-M to test the ability of the IBW antennas to exert a PF on the plasma, and this experiment has been simulated by incorporating the equilibrium ponderomotive force into the TSC code. The simulation predicts that a modulated PF of the proper amplitude and phase can counter the magnetic axis shift induced by a vertical field modulation for a reasonable set of PBX-M experimental parameters.

This work was supported by US Department of Energy Contracts Nos. DE-AC020-76-CHO3073, DE-F605-80ET-53088, W-7405-ENG-36, and DE-FG05-93ER-81587.

REFERENCES

- [1] CONN, R.W., NAJMABADI, F., in *Plasma Physics and Controlled Nuclear Fusion Research 1990* (Proc. 13th Int. Conf. Washington, DC, 1990), Vol. 3, IAEA, Vienna (1991) 659.
- [2] CHANCE, M.S., et al., *ibid.*, Vol. 2, p. 87.
- [3] KESSEL, C.E., et al., *Phys. Rev. Lett.* **72** (1994) 1212.
- [4] CHANCE, M.S., et al., in *Proc. 15th Int. Conf. on the Numerical Simulation of Plasmas*, Valley Forge, PA, 1994.
- [5] BONDESON, A., WARD, D.J., *Phys. Rev. Lett.* **72** (1994) 2709.
- [6] POGUTSE, O.P., YURCHENKO, E.I., *Sov. J. Plasma Phys.* **3** (1977) 283.
- [7] GIMBLETT, C.G., *Nucl. Fusion* **26** (1986) 617.
- [8] BONDESON, A., PERSSON, M., *Nucl. Fusion* **28** (1988) 1887.
- [9] FINN, J.M., *Phys. Plasmas* **2** (1995) 198.
- [10] FITZPATRICK, R., HASTIE, R.J., MARTIN, T.J., ROACH, C.M., *Nucl. Fusion* **33** (1993) 1533.
- [11] D'IPPOLITO, D.A., *Phys. Fluids* **31** (1988) 340;
D'IPPOLITO, D.A., GOEDBLOED, J.P., *Phys. Fluids B* **1** (1989) 804;
GOEDBLOED, J.P., D'IPPOLITO, D.A., *Phys. Fluids B* **2** (1990) 2366.

DISCUSSION

J.A. WESSON: What is the relation of your 'mantle' to the real situation in which the scrape-off layer is much narrower than the plasma-wall separation?

N. POMPHREY: The existence of a mantle is not essential to the viscous/inertia stabilization mechanism, as may be seen particularly in the analytical results of R. Fitzpatrick (IAEA-CN-60/D-5), who obtains stabilization even in a vacuum. In the resistive external kink stabilization, resistivity is only needed up to the location of the tearing layer region formed at the rational surface.

M.G. HAINES: Did you use isotropic or anisotropic viscosity for the magnetized plasma?

N. POMPHREY: We used a simple isotropic viscosity model with $F_{\text{viscosity}} = \nabla \times \mu \nabla \times v$ in the momentum equation of motion.

M.G. HAINES: Did you use a realistic value for viscosity?

N. POMPHREY: The value for viscosity, μ , was chosen in accordance with the observed anomalous values at the edge of tokamak plasmas. In terms of momentum diffusivity, the value corresponds to $10 \text{ m}^2/\text{s}$.